the FEBS Journal

Bistability from double phosphorylation in signal transduction

Kinetic and structural requirements

Fernando Ortega[1,2,3], José L. Garcés[1,2], Francesc Mas[1,2], Boris N. Kholodenko[4] and Marta Cascante[1,3]

1 Centre for Research in Theoretical Chemistry, Scientific Park of Barcelona, Spain
2 Physical Chemistry Department, University of Barcelona, Spain
3 Department of Biochemistry and Molecular Biology, University of Barcelona, Spain
4 Department of Pathology, Anatomy and Cell Biology, Thomas Jefferson University, Philadelphia, PA, USA

Keywords
bistability; metabolic cascades; signaling networks; ultrasensitivity

Correspondence
M. Cascante, Department of Biochemistry and Molecular Biology, University of Barcelona and Centre for Research in Theoretical Chemistry, Scientific Park of Barcelona, Marti i Franquès 1, 08028 Barcelona, Spain
Fax: +34 93 402 12 19
Tel: +34 93 402 15 93
E-mail: martacascante@ub.edu

Note
The mathematical model described here has been submitted to the Online Cellular Systems Modelling Database and can be accessed free of charge at http://jjj.biochem.sun.ac.za/database/Ortega/index.html

(Received 19 February 2006, revised 13 June 2006, accepted 23 June 2006)

doi:10.1111/j.1742-4658.2006.05394.x

Previous studies have suggested that positive feedback loops and ultrasensitivity are prerequisites for bistability in covalent modification cascades. However, it was recently shown that bistability and hysteresis can also arise solely from multisite phosphorylation. Here we analytically demonstrate that double phosphorylation of a protein (or other covalent modification) generates bistability only if: (a) the two phosphorylation (or the two dephosphorylation) reactions are catalyzed by the same enzyme; (b) the kinetics operate at least partly in the zero-order region; and (c) the ratio of the catalytic constants of the phosphorylation and dephosphorylation steps in the first modification cycle is less than this ratio in the second cycle. We also show that multisite phosphorylation enlarges the region of kinetic parameter values in which bistability appears, but does not generate multistability. In addition, we conclude that a cascade of phosphorylation/dephosphorylation cycles generates multiple steady states in the absence of feedback or feedforward loops. Our results show that bistable behavior in covalent modification cascades relies not only on the structure and regulatory pattern of feedback/feedforward loops, but also on the kinetic characteristics of their component proteins.

One of the major challenges in the postgenomic era is to understand how biological behavior emerges from the organization of regulatory proteins into cascades and networks [1,2]. These signaling pathways interact with one another to form complex networks that allow the cell to receive, process and respond to information [3].

One of the main mechanisms by which signals flow along pathways is the covalent modification of proteins by other proteins. Goldbeter & Koshland showed that this multienzymatic mechanism could display ultrasensitive responses, i.e. strong variations in some system variables, to minor changes in the effector controlling either of the modifying enzymes [4,5]. In the same way, a double modification cycle represents an alternative mechanism that enhances switch-like responses [6,7]. However, it has been reported that, in systems where covalent modification is catalyzed by the same bifunctional enzyme rather than by two independent

Abbreviation
M-M, Michaelis–Menten.

proteins, this modification cycle does not generate large responses. The adenylylation/deadenylylation of glutamine synthetase catalysed by adenylyltransferase is an example [8].

Switch-like behavior, often displayed by cellular pathways in response to a transient or graded stimulus, can be either ultrasensitive [4] or true switches between alternate states of a bistable system [9]. It has been posited that bistability contributes to processes such as differentiation and cell cycle progression [1,10]. It may also produce dichotomous responses and a type of biochemical memory [1,9]. Bistability may arise from the way the signal transducers are organized into signaling circuits. Indeed, feedback in various forms (i.e. positive feedback, double-negative feedback or autocatalysis) has been described as a necessary element for bistability, although it does not guarantee this [11–15].

The question arises as to whether bistability can be generated by mechanisms other than those already described in the literature. Recently, it has been shown that in two-step modification enzyme cycles, in which the two modification steps or the two demodification steps are catalyzed by the same enzyme, bistability can be generated [16]. However, an analytic study of the conditions that the parameters must fulfill in order to obtain bistability behavior is still lacking.

The present article analytically demonstrates that both dual and multisite modification cycles can display bistability and hysteresis. We work out the key quantitative relationships that the kinetic parameters must fulfill in order to display a true switch behavior. First, we analyze a two-step modification cycle with a nonprocessive, distributive mechanism for the modifier and demodifier enzymes and obtain analytically the kinetic constraints that result in bistable behavior as well as the region of kinetic parameter values in which two stable steady states can coexist. Second, we show that a multimodification cycle of the same protein does not introduce more complex behavior, but rather enlarges the kinetic parameter values region in which bistability appears. We also show that multistability can arise from modification cycles organized hierarchically without the existence of any feedback or feedforward loop, i.e. when the double-modified protein catalyzes the double modification of the second-level protein.

Finally, using the quantitative kinetic relationships explained in the present article, we identify the MAPKK1-p74raf-1 unit in the MAPK cascade as a candidate for generating bistable behavior in a signal transduction network, in agreement with the kinetic characteristics reported in the literature [17].

The mathematical model described here has been submitted to the Online Cellular Systems Modelling Database and can be accessed free of charge at http://jjj.biochem.sun.ac.za/database/Ortega/index.html

1. Two-step modification cycles

Initially, let us consider a generic protein W, which is covalently modified on two residues in a modification cycle that occurs through a distributive mechanism. For the sake of simplicity, we investigate the case in which the order of the modifications is compulsory (ordered).

Figure 1 shows a two-step modification enzyme cycle in which both modifier and demodifier enzymes, e_1 and e_2, follow a strictly ordered mechanism. As illustrated, the interconvertible protein W only exists in three forms: unmodified (W_α), with one modified residue (W_β) and with two modified residues (W_γ). The four arrows represent the interconversion between these three different forms: $W_\alpha \rightarrow W_\beta$ (step 1), $W_\beta \rightarrow W_\alpha$ (step 2), $W_\beta \rightarrow W_\gamma$ (step 3) and $W_\gamma \rightarrow W_\beta$ (step 4). In order to simplify the analysis, it is also assumed that each of the four interconversions follows a Michaelis–Menten (M-M) mechanism [18]:

$$W_S + e \underset{k_{di}}{\overset{k_{ai}}{\rightleftarrows}} eW_S \xrightarrow{k_i} W_P + e$$

where k_{ai}, k_{di} and k_i are the association, dissociation and catalytic constants, respectively, of step *i*. eW_S is the M-M complex formed by the catalyst, e, and its substrate, W_S, to produce the product, W_P, where W_S and W_P are two forms of the interconvertible protein W. It is also assumed that the other substrates and products (for instance, ATP, P_i and ADP in the case of a phosphorylation cascade) are present at constant levels and, consequently, are included in the kinetic constants.

For the metabolic scheme depicted in Fig. 1, steps 1 and 3 are catalyzed by the modifying enzyme (e_1), whereas the second and fourth steps are catalyzed by

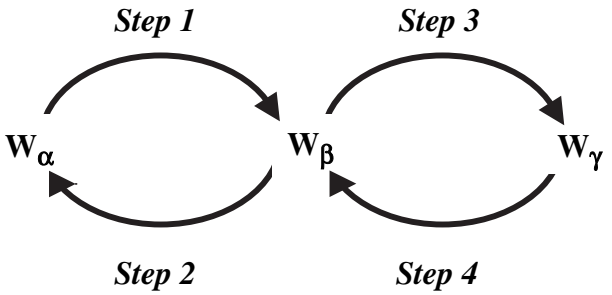

Fig. 1. Kinetic diagram, in which a protein W has three different forms W_α, W_β and W_γ. The four arrows show the interconversion between the different forms: $W_\alpha \rightarrow W_\beta$ (step 1); $W_\beta \rightarrow W_\alpha$ (step 2); $W_\beta \rightarrow W_\gamma$ (step 3); and $W_\gamma \rightarrow W_\beta$ (step 4). Steps 1 and 3 are catalyzed by the same enzyme (e_1), and steps 2 and 4 are catalyzed by another enzyme (e_2).

the demodifying enzyme (e_2). Under the steady-state assumption, the rate equations (v_i) have the following form for the four steps (see Appendix A):

$$v_1 = \frac{V_{m1}\frac{\alpha}{K_{S1}}}{1+\frac{\alpha}{K_{S1}}+\frac{\beta}{K_{S3}}} \quad v_3 = \frac{V_{m3}\frac{\beta}{K_{S3}}}{1+\frac{\alpha}{K_{S1}}+\frac{\beta}{K_{S3}}}$$
$$v_2 = \frac{V_{m2}\frac{\beta}{K_{S2}}}{1+\frac{\gamma}{K_{S4}}+\frac{\beta}{K_{S2}}} \quad v_4 = \frac{V_{m4}\frac{\gamma}{K_{S4}}}{1+\frac{\gamma}{K_{S4}}+\frac{\beta}{K_{S2}}} \qquad (1)$$

where $\alpha = [W_\alpha]/W_T$, $\beta = [W_\beta]/W_T$ and $\gamma = [W_\gamma]/W_T$ are the dimensionless concentrations of species W_α, W_β and W_γ, and W_T is the total concentration of the interconvertible protein W; $K_{Si} = K_{mi}/W_T$, where K_{mi} $[(k_{di} + k_i)/k_{ai}]$ is the Michaelis constant and V_{mi} $(k_i e_{fT}, i = 1, 4)$ is the maximal rate of step i where $j = 1$ for $i = 1, 3$ and $j = 2$ for $i = 2, 4$. For convenience, we define: $r_{31} = V_{m3}/V_{m1} = k_3/k_1$, $r_{24} = V_{m2}/V_{m4} = k_2/k_4$ and $\chi_{14} = V_{m1}/V_{m4} = (k_1/k_4)(e_{1T}/e_{2T}) = r_{14}T_{12}$. Note that r_{31} and r_{24} are the ratios of the catalytic constants for the modification and demodification processes, respectively, and are therefore independent of the enzyme concentrations. In contrast, the ratio χ_{14} depends on the enzyme concentrations ratio ($T_{12} = e_{1T}/e_{2T}$) and the ratio of the catalytic constants r_{14} of the first modification and the first demodification steps, i.e. the ratio between maximal activities of the first and fourth steps.

2. Bistability in double modification cycles

The differential equations that govern the time evolution of the system shown in Fig. 1 are:

$$\frac{dW_\alpha}{dt} = W_T\frac{d\alpha}{dt} = v_2 - v_1$$
$$\frac{dW_\beta}{dt} = W_T\frac{d\beta}{dt} = v_1 - v_2 - v_3 + v_4 \qquad (2)$$
$$\frac{dW_\gamma}{dt} = W_T\frac{d\gamma}{dt} = v_3 - v_4$$

Assuming the pseudo-steady state for the enzyme-containing complexes, these equations together with the conservation relationships (see Appendix A) and the initial conditions allow us to determine the concentrations of all forms of the interconvertible protein as functions of time. In the system's steady state, $v_1 = v_2 \equiv j_1$ and $v_3 = v_4 \equiv j_3$.

In order to derive analytically the set of parameter values at which the system qualitatively changes its dynamic behavior from one to three steady states, we first analyze a plot of the mole fraction α at steady state as a function of the ratio χ_{14} for two different values of the product of $r_{31}r_{24}$ at fixed K_S values (Fig. 2). This product is called the asymmetric factor (Θ) and is the ratio of the product of the catalytic constants of the steps that consume (k_3k_2) and the steps that produce the species W_β (k_1k_4). At low Θ value, there is a single stable steady state for any value of χ_{14} (curve (A) in Fig. 2). However, for a larger value of asymmetric factor (Θ), there is a range of χ_{14} values at which three steady states are possible, two of which are stable and one unstable (shown by the dashed line in curve (B) of Fig. 2). Thus, this model can present three steady states for the same set of parameters, even in the absence of allosteric mechanisms such as a positive feedback loop. In the following, a critical set of parameter values that induces a transition from one to three steady states (i.e. bifurcation point) will be determined.

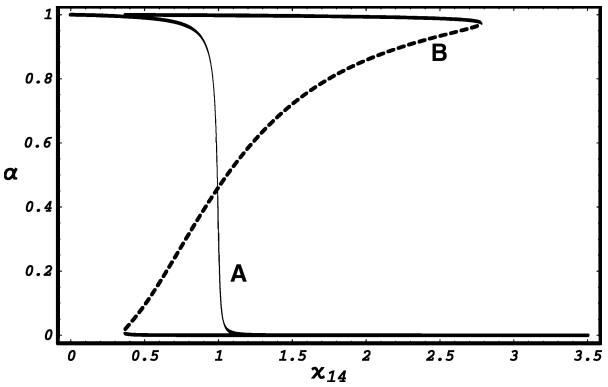

Fig. 2. Effect of the asymmetric factor Θ ($r_{31}r_{24}$) on the steady-state molar fraction α as a function of χ_{14} for a fixed $K_S = 10^{-2}$ for the model. The parameters considered are: $\Theta = 1$ ($r_{31} = r_{24} = 1$) and 36 ($r_{31} = r_{24} = 6$) for curves (A) and (B), respectively.

To obtain the steady state, Eqn (2) was equated to zero. Since the denominators of Eqn (1) are equal, the relationship $v_1/v_3 = v_2/v_4$ yields:

$$\frac{K_{S2}K_{S3}}{K_{S1}K_{S4}}\frac{\alpha\gamma}{\beta^2} = r_{31}r_{24} \equiv \Theta \qquad (3)$$

This relationship imposes strong restrictions on the values of the molar fractions α, β and γ at the steady state.

For the sake of simplicity, we consider initially that the total concentration of the interconvertible protein, W_T, is much larger than e_{T1} and e_{T2} and that, consequently, the M-M complexes can be ignored. Under this condition, the conservation relations give $\beta = 1 - \alpha - \gamma$.

Assuming that the Michaelis constants of the modifier and demodifier enzymes are equal, namely, $K_{S1} = K_{S3}$ and $K_{S2} = K_{S4}$, and considering Eqn (2) and Eqn (3), the following mathematical expressions for α, β and χ_{14} can be expressed as a function of γ, the asymmetric factor ($\Theta = r_{31}r_{24}$), K_{S1} and K_{S2}:

$$\alpha = \frac{(-\gamma + \sqrt{\gamma^2 + 4\gamma\Theta - 4\gamma^2\Gamma\Theta})^2}{4\gamma\Theta}$$
$$\beta = \frac{-\gamma + \sqrt{\gamma^2 + 4\gamma\Theta - 4\gamma^2\Theta}}{2\Theta} \quad (4)$$
$$\chi_{14} = \frac{\beta\gamma + \beta^2\Theta + \gamma K_{S1}}{\beta r_{31}(\beta + \gamma + K_{S2})}$$

This last equation shows how χ_{14} depends on γ and permits us to calculate the bifurcation point. When the system displays a single steady state, the χ_{14} value increases monotonically with γ, i.e. $\partial\gamma/\partial\chi_{14} > 0$. In contrast, when the system shows bistable behavior, the slope of this curve has a different sign depending on the range of γ values. Therefore, the curve has two extrema and an inflection point (Fig. B1 in Appendix B). At the bifurcation point, a change in the qualitative behavior of the system occurs and the following constraints are satisfied (this way of calculating the bifurcation point is equivalent to linearizing the system defined by Eqn (2) around the steady state and calculating the set of parameter values for which one of the eigenvalues is equal to zero and its derivative with respect to χ_{14} is positive; this latter condition ensures that any χ_{14} increases provoke the loss of stability of the solution):

$$\left(\frac{\partial\chi_{14}}{\partial\gamma}\right) = 0 \quad \text{and} \quad \left(\frac{\partial^2\chi_{14}}{\partial\gamma^2}\right) = 0 \quad (5)$$

In the following subsections, we solve the equations presented above and analyze the consequences derived from them.

2.1. Bifurcation point analysis in the case of equal Michaelis constants of modifier and demodifier enzymes

For the sake of simplicity, let us assume that the Michaelis constants of both enzymes are equal, namely $K_{S1} = K_{S2} = K_S$. Introducing Eqn (4) into Eqn (5), it can be shown, after some algebra, that the asymmetric factor at the bifurcation point must satisfy the following equation:

$$\Theta \equiv r_{31}r_{24} = \frac{k_3k_2}{k_1k_4} = \frac{(1 + K_S)^2}{(1 - 2K_S)^2} \quad \text{and} \quad K_S < 1/2 \quad (6)$$

Thus, for any set of parameters such that Θ is larger than the threshold value given in Eqn (6) and K_S lower than 1/2, there is a region of χ_{14} values in which two stable steady states coexist. However, when Θ is lower than the value given by Eqn (6) or when K_S is greater than 1/2, the system has only one steady state. The variation of Θ with K_S is shown in Fig. 3. It should be noted that when K_S tends asymptotically to zero, the value of Θ needed to satisfy the bifurcation point condition tends to 1, whereas when K_S tends to 1/2, this value tends asymptotically to infinity. In other words, if the Michaelis constants of modifier and demodifier are equal, a necessary condition for the system to display bistability behavior is that the product of the catalytic constants of the modification and demodification of the form W_β should be greater than the product of the catalytic constant of W_α modification and W_γ demodification enzymes.

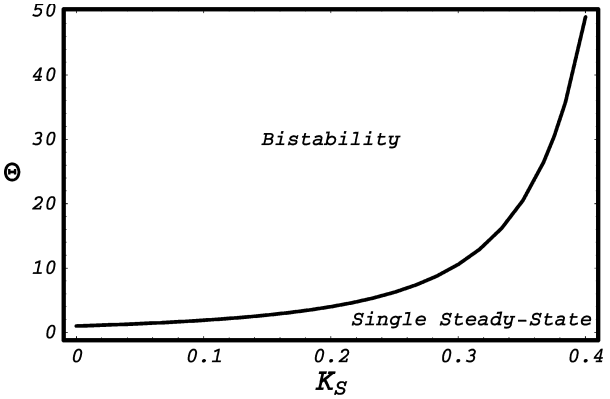

Fig. 3. Variation of the asymmetric factor Θ ($r_{31}r_{24}$) with the Michaelis constant ($K_{S1} = K_{S2} = K_S$) at the bifurcation point.

By substituting Eqn (6) into Eqn (2) and Eqn (4), analytic expressions for the system variables, α, β and γ are obtained. In particular, at the bifurcation point, it follows that:

$$\chi_{14} = r_{24}\frac{1 - 2K_S}{1 + K_S} = \sqrt{\frac{r_{24}}{r_{31}}} \quad (7)$$

Interestingly, at the bifurcation point, χ_{14} takes a value that depends on the ratio between the product of the catalytic constant of cycle 1 (steps 1 and 2) and cycle 2 (steps 3 and 4) (Eqn 7) and the values of α, γ and β only depend on the K_S value (Eqn 8). The concentrations of interconvertible forms are:

$$\gamma = \alpha = \frac{1 + K_S}{3} \quad \text{and} \quad \beta = \frac{1 - 2K_S}{3} \quad (8)$$

The flux values of cycle 1 and cycle 2 are:

$$j_1 = r_{24}\frac{1 - 2K_S}{1 + K_S}\frac{V_{m4}}{2} = \sqrt{\frac{r_{24}}{r_{31}}}\frac{V_{m4}}{2} \quad \text{and} \quad j_3 = \frac{V_{m4}}{2} \quad (9)$$

Also, at the bifurcation, the α values and γ values are equal. On the other hand, the lower the K_S value, the more $\alpha(=\gamma)$ and β values tend towards 1/3; and as K_S approaches 1/2, α $(=\gamma)$ tends to 1/2, whereas β tends to 0. Thus, the values of the different species of the interconvertible protein W at the bifurcation point

are constrained: α and γ only vary between 1/3 and 1/2, whereas β varies between 0 and 1/3.

2.2. Bifurcation point analysis when Michaelis constants of modifier and demodifier enzymes differ

Equations (6), (7), (8) and (9) were obtained under the assumption that all the Michaelis constants of the two modifier enzymes were equal to K_S. Here we consider the more general situation in which the Michaelis constants of the modifier and demodifier enzymes are different. K_{S1} and K_{S2} are the dimensionless Michaelis constants for the reactions catalyzed by the enzymes e_1 and e_2, respectively. For this more general case, at the bifurcation point the analytic expression for Θ in terms of K_{S1} and $\rho = K_{S2}/K_{S1}$ was derived (see supplementary Doc. S1A). From this expression, it turns out that the value of Θ is always higher than 1. The dependence of Θ on K_{S1} and ρ is displayed in Fig. 4, showing that two regions can be defined in the space of kinetic parameters (ρ, K_{S1}), one resulting in bistable behavior and the other resulting in a single stable steady state. The border between these two regions corresponds to the following curve (see supplementary Doc. S1A):

$$\rho = -\frac{1 + K_{S_1}}{K_{S_1}(1 - 8K_{S_1})} \qquad (10)$$

3. Double modification cycles: numerical examples

In the previous section, we analyzed the necessary conditions for bistability. In this section, the same system is studied for different sets of parameters, resulting in (a) a single steady state and (b) bistable behavior.

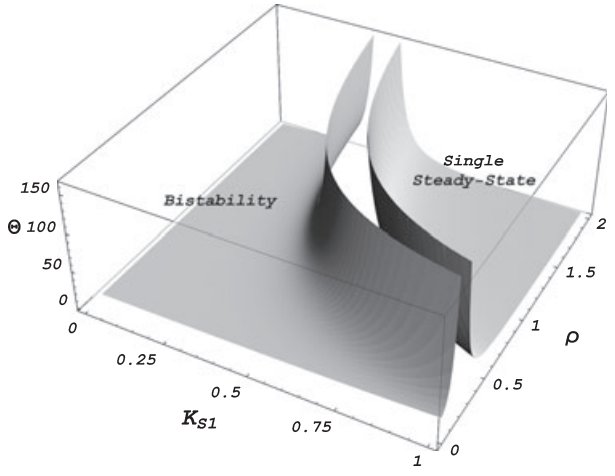

Fig. 4. Dependence of the asymmetric factor (Θ) at the bifurcation point on K_{S1} and ρ (= K_{S2}/K_{S1}).

3.1. Parameter restrictions for a stable steady state

To analyze monostable behavior, we chose a set of parameter values $K_S = K_{S1} = K_{S2}$, r_{31} and r_{24}, such that the asymmetric factor obeys the restriction $\Theta < (1 + K_S)^2/(1 - 2K_S)^2$, and $K_S < 1/2$. As sensitivity is enhanced with the decrease of K_S in an interconvertible protein system [4], a value of $K_S = 10^{-2}$ was selected. The corresponding value of the asymmetric factor, calculated using Eqn (6), is 1.06 at the bifurcation point.

Figure 5 shows the dependence of α, β, γ and the cycle fluxes on the χ_{14} for the same K_S, but different values of the asymmetric factor. From the curves displayed in Fig. 5A,B, ultrasensitivity clearly depends not only on the K_S value but also on the asymmetric factor. The closer the Θ value to the value given by Eqn (6), the steeper the change in the molar fraction value of α and γ with respect to χ_{14}. In particular, for $\Theta = 1$ there is an abrupt decrease of α in parallel with an increase in γ and flux through cycle 2. β and flux through cycle 1 increase and then abruptly decrease in parallel with the decrease in α (Fig. 5C,D,E).

β attains its maximal value (β_{max}) at $\chi_{14} = \sqrt{(r_{24}/r_{31})}$, and β_{max} depends only on the asymmetric factor $\beta_{max} = 1/(1 + 2\sqrt{\Theta})$. At β_{max} the concentrations of the other forms α and γ are as follows: $\alpha = \gamma = \sqrt{\Theta}/(1 + 2\sqrt{\Theta})$ (see supplementary Doc. S1B for their derivation).

3.2. Parameter restrictions that allow bistability

For the bistable case, we chose a set of parameter values, K_S, r_{31} and r_{24}, such that the asymmetric factor satisfies the restriction $\Theta > (1 + K_S)^2/(1 - 2K_S)^2$, and $K_S < 1/2$. For all the values of Θ that obey the above inequalities, there exists an interval of χ_{14} values in which two stable steady states coexist together with an unstable steady state, as shown in Fig. 6 for $K_S = 10^{-2}$ and various Θ values.

It should be noted that the unstable steady state for α and γ always lies in between the two stable states, whereas the unstable steady state for β is always higher than the two stable steady states (Fig. 6A–C). Application of the same reasoning as in the previous section demonstrates that β_{max}, which always corresponds to the unstable steady state, decreases with the increase of the asymmetric factor and occurs at $\chi_{14} = \sqrt{(r_{24}/r_{31})}$ (see also supplementary Doc. S1B). Note that in

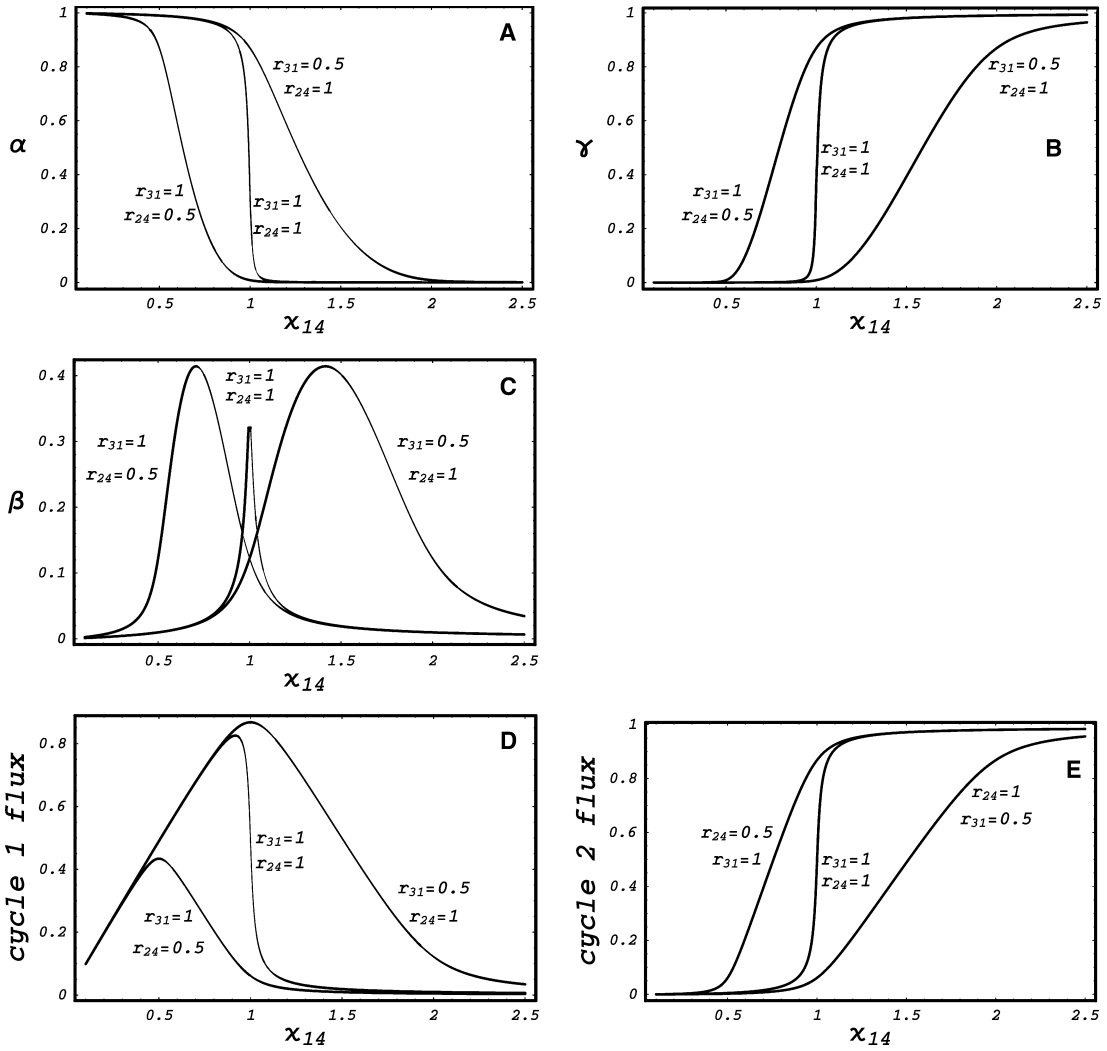

Fig. 5. The effect of the ratios of the catalytic constants ($r_{31} = k_3/k_1$ and $r_{24} = k_2/k_4$) on the variation of the steady-state variable profiles with χ_{14}, at a fixed K_S value ($K_S = 10^{-2}$). (A), (B) and (C) show the molar fractions α ($[W_\alpha]/W_T$), β ($[W_\beta]/W_T$) and γ ($[W_\gamma]/W_T$) as a function of χ_{14}, respectively. (D) and (E) show the steady-state fluxes of cycles 1 and 2 as a function of χ_{14}. The kinetic parameter values considered, indicated in the plots, correspond to asymmetric factor values $\Theta = r_{31}r_{24} = 0.5$ and 1. Note that $\Theta = 0.5$ corresponds to two different cases: $r_{31} = 0.5$, $r_{24} = 1$ and $r_{31} = 1$, $r_{24} = 0.5$.

Fig. 6C the maximum of the three curves appears at the same position because for the three curves $r_{24}/r_{31} = 1$.

Figure 6D,E shows that at the unstable steady-state cycle, the fluxes of cycle 1 and 2 are comparable, whereas the two stable steady-state fluxes correspond to two extreme situations, in which only one of the cycles is active and practically no flux goes through the other cycle.

Finally, we analyzed how the asymmetric factor and parameter values determine the range of χ_{14} values that correspond to the bistability domain. The dependence of χ_{14} on γ gives two extrema points. The difference between them determines the range of bistable behavior. The dependence of this interval on Θ and r_{24} follows a complex explicit expression. The variation of the amplitude of this interval with the asymmetric factor at different values of r_{24} is shown in Fig. 7. For each value of r_{24} there is a value of Θ that maximizes the bistability interval; this maximum value increases when r_{24} increases. In addition, this range increases monotonically when K_S decreases (data not shown).

An approximate expression for the bistability interval in terms of the main enzyme's kinetic parameters can be obtained. When the molar fraction α is close to 1, the stationary flux of cycle 1 varies linearly with χ_{14}, because the enzyme of step 1 is saturated (see

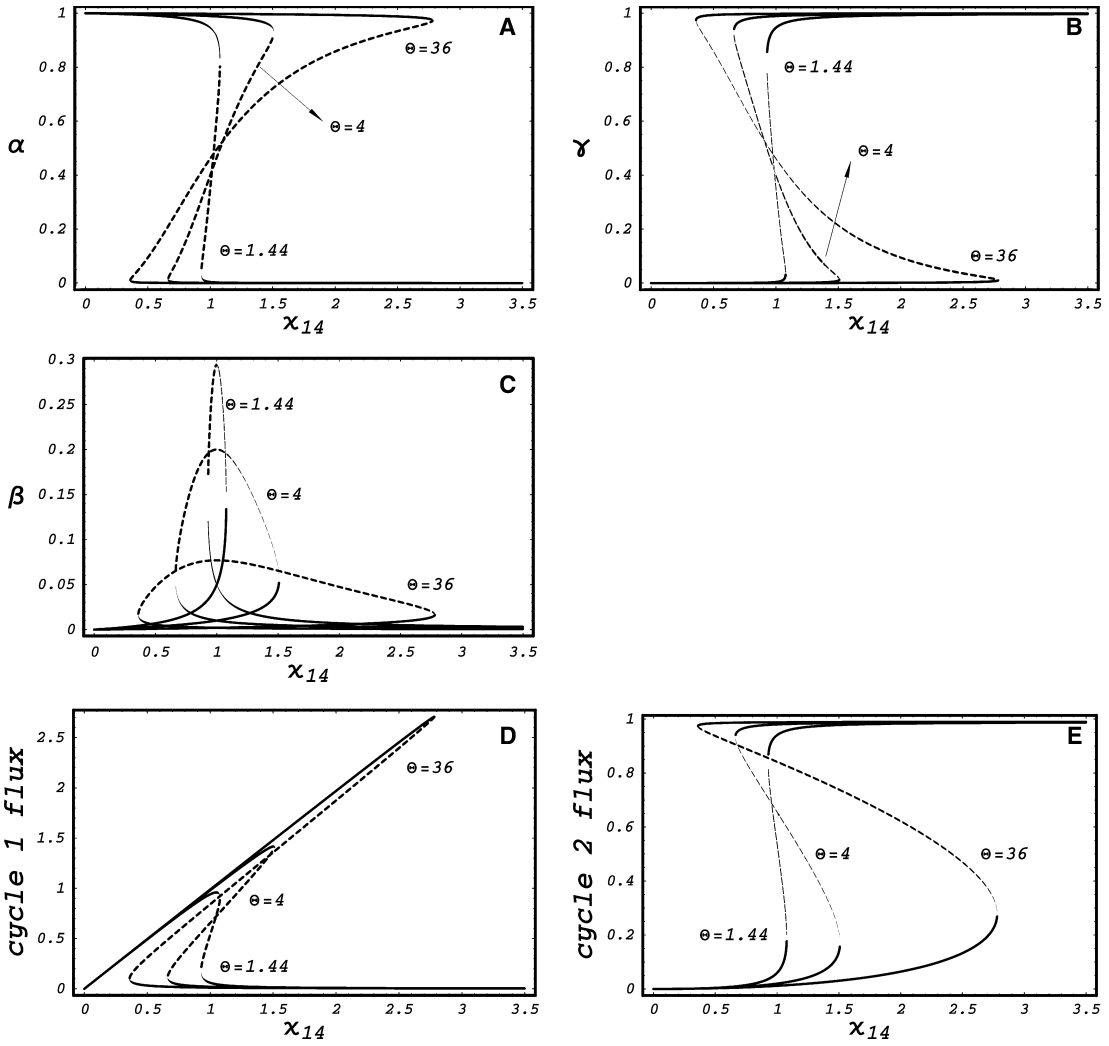

Fig. 6. The effect of the value of the asymmetric factor (Θ) on the variation of the steady-state variable profiles with χ_{14}, at a fixed K_S value ($K_S = 10^{-2}$) and $r_{31} = r_{24}$. (A), (B) and (C) show the molar fractions α ($[W_\alpha]/W_T$), β ($[W_\beta]/W_T$) and γ ($[W_\gamma]/W_T$) as functions of χ_{14}, respectively. (D) and (E) show the steady-state fluxes of cycles 1 and 2 as a function of χ_{14}. As $r_{31} = r_{24}$, the χ_{14} value at which β rises to its maximum value (β_{max}) is $\sqrt{r_{24}/r_{31}} = 1 \ = 1$ (see Section 3.1).

Fig. 6D). Thus, from Eqn (1), this flux can be approximated by $j_1 \approx V_{m1} \approx V_{m2}\beta/(K_S + \beta)$, since $\alpha >> \beta$ and γ is negligible while cycle 1 controls the flux. On rearranging the above expression, a relationship between χ_{14} and β is obtained: $\beta = K_S \chi_{14}/(r_{24} - \chi_{14})$. Conversely, when the molar fraction α is close to 0, the approximate expression obtained is $\beta \approx K_S/(\Theta\ \chi_{14}/r_{24} - 1)$. Since the molar fraction β must be between 0 and its maximum value (Eqn 8), the above expressions give an estimate for the extrema points. Then, an estimate of the range of bistability can be given by $r_{24}\,(1 + K_S)/[\Theta\,(1 - 2\,K_S)] < \chi_{14} < r_{24}\,(1 - 2\,K_S)/(1 + K_S)$, which yields a wider range than the exact calculation.

4. Bistability and multistability in systems of multimodified proteins

This section analyzes the minimal structural changes that need to be introduced into a two-step modification enzyme cycle in order to generate multistability, assuming simple M-M mechanisms. We consider two types of structural change: (a) an increase in the number of cycles, and (b) the introduction of a hierarchical organization, as in MAP kinase cascades.

It might seem, *a priori*, that if a two-step modification enzyme cycle can generate bistability, an interconvertible protein with multisite modification will generate multistability when the modifier or demodifier

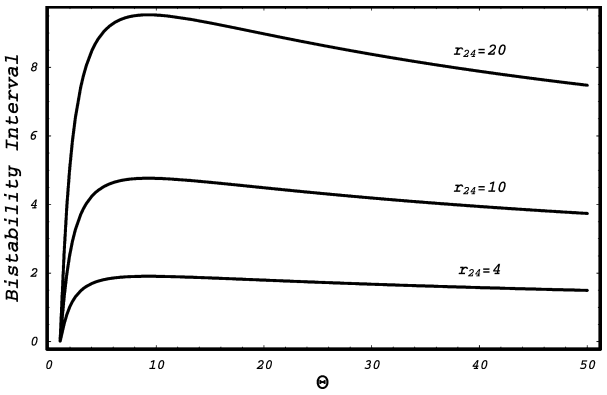

Fig. 7. Existence of an optimal r_{31} value for a given set of parameters r_{24} and K_S, which maximizes the range of bistability. The value of the parameters considered are $r_{24} = 4$, 10, 20 and $K_S = 10^{-2}$.

steps are catalyzed by the same enzyme (Fig. 8A). As shown below, this assumption is not true: additional modification steps catalyzed by the same enzyme do not lead to multistability. Therefore, we considered the addition of cycles at different levels of an enzyme cascade. For example, a couple of two-step modifier/demodifier cycles can be organized such that the modification steps of the first interconvertible protein (W) are catalyzed by the same enzyme, and its double-modified form (W_γ) catalyzes the modification steps of a second interconvertible enzyme (Z) (Fig. 8B).

4.1. More than two consecutive modifications of a multisite interconvertible protein

We consider an interconvertible protein (W) that can exist in four different modification forms, W_α, W_β, W_γ and W_δ (e.g. different phosphorylation states). The modification and demodification steps are catalyzed by the enzymes e_1 and e_2, respectively (Fig. 8A). The rate equations are derived in a similar way to the double modification case (Appendix A). The molar fractions of the different forms of the interconvertible protein are α, β, γ and δ. For convenience, we introduce the five following combinations of parameters: $r_{31} = V_{m3}/V_{m1} = k_3/k_1$, $r_{53} = V_{m5}/V_{m3} = k_5/k_3$, $r_{24} = V_{m2}/V_{m4} = k_2/k_4$, $r_{46} = V_{m4}/V_{m6} = k_4/k_6$ and $\chi_{16} = V_{m1}/V_{m6} = (k_1/k_6)(e_{1T}/e_{2T}) = r_{16}T_{12}$, where the k_i values with $i = 1$–6 are the different catalytic constants of the respective steps, and e_{T1} and e_{T2} are the total concentrations of the modifier/demodifier enzymes, respectively. For this interconvertible protein, analytic expressions for the bifurcation points, using the same methodology applied in Section 2, were not found. Numerical simulations that were conducted for a broad set of parameter values for the relationships

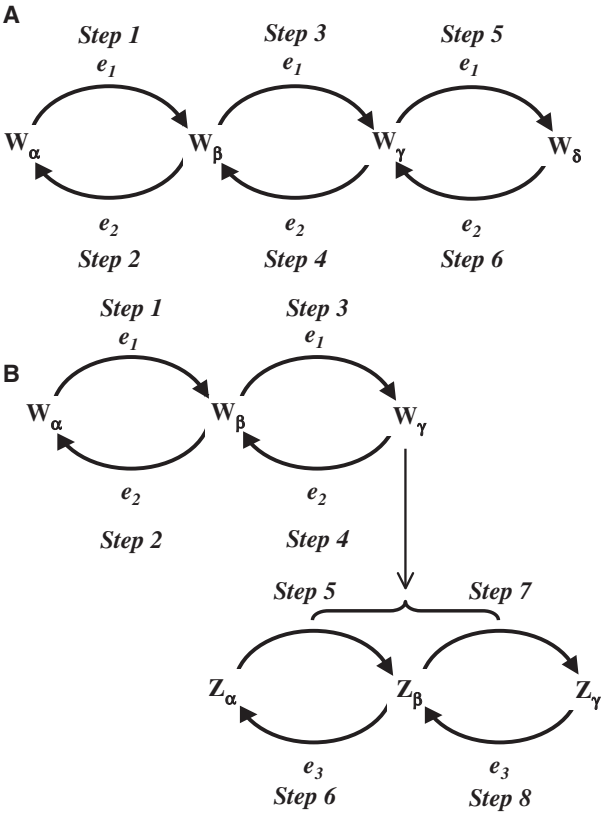

Fig. 8. (A) Diagram with four different protein W forms, W_α, W_β, W_γ and W_δ. The arrows show the interconversion between the forms: $W_\alpha \rightarrow W_\beta$ (step 1); $W_\beta \rightarrow W_\alpha$ (step 2); $W_\beta \rightarrow W_\gamma$ (step 3); $W_\gamma \rightarrow W_\beta$ (step 4); $W_\gamma \rightarrow W_\delta$ (step 5); and $W_\delta \rightarrow W_\gamma$ (step 6). Steps 1, 3 and 5 are catalyzed by the same enzyme (e_1). The second, fourth and sixth steps are catalyzed by another enzyme (e_2). (B) Network diagram with two interconvertible proteins W and Z. Each protein has three different forms, W_α, W_β, W_γ, and Z_α, Z_β, Z_γ, respectively. The modification and demodification steps of protein W are catalyzed by e_1 and e_2, respectively. The modification steps of protein Z are catalyzed by the active form of the protein W (W_γ), and the demodification steps are catalyzed by the enzyme e_3.

r_{31}, r_{53}, r_{24} and r_{46} showed that the system does not present more than two stable steady states for a given χ_{16} (result not shown). In a particular case, i.e. when the Michaelis constants are equal and the relationship $r_{31}r_{24} = r_{53}r_{46}$ holds, an analytic expression for the bifurcation point can be found. Using the same methodology developed in Section 2, the bifurcation point occurs at:

$$\Theta = r_{31}r_{24} = \frac{1 + K_s}{1 - K_s} \quad \text{and} \quad K_s < 1 \qquad (11)$$

Consequently, for a given value of K_S lower than 1, the system has bistable and hysteresis behavior if the asymmetric factor is greater than the one given by Eqn (11) [$\Theta > (1 + K_S)/(1 - K_S)$]. Moreover, the

concentrations of the different species of the interconvertible protein W at the bifurcation point are:

$$\alpha=\delta=\frac{1+K_s}{4},\ \beta=\gamma=\frac{1-K_s}{4} \quad \text{and} \quad \chi_{16}=r_{31}r_{24} \quad (12)$$

To compare this particular case with the two-step modification cycle (Section 2.1), we assume that $r_{31} = r_{24}$. In this case, the bifurcation point expressions for the triple and double covalent modification systems are $r_{31} = (1 + K_S)/(1 - 2K_S)$ and $r_{31} = \sqrt{(1 + K_S)}/(1 - K_S)$, respectively. These expressions show that the triple cycle (Fig. 8A) requires less restrictive constraints on parameter values than the double cycle (Fig. 1). Thus, at the same K_S value, bistability is achieved in the triple cycle at a lower r_{31} value than in the double cycle. Moreover, the interval at which bistability appears is longer for the triple cycle system than for the double cycle system.

4.2. A cascade of two modifier/demodifier cycles can generate multistable behavior

As shown in the previous section, the modification of multiple sites of a protein by the same enzyme does not generate more complex behavior than bistability. Here, we explore the possibility that a cascade of two double modification cycles, following simple M-M kinetics, generates multistability. We consider a system of two modifier/demodifier cycles (Fig. 8B), such that the double modification of the first interconvertible protein (W) is catalyzed by the same enzyme, and the double modified form (W_γ) catalyzes the double modification of a second interconvertible enzyme (Z). We assume that the double-modified protein (W_γ) is the only form of the interconvertible enzyme W that has catalytic activity. The demodifications of the interconvertible proteins W and Z are catalyzed by independent and constitutively active enzymes e_2 and e_3, respectively. In the appropriate range of kinetic parameters and interconvertible protein concentrations, this system can generate up to five different steady states, three of which are stable and the other two unstable (see supplementary Fig. S1). The system has five steady states only if each double modification cycle operates in the same range in which it individually displays bistable behavior.

5. Discussion

The recognition that bistable switching mechanisms trigger crucial cellular events, such as cell cycle progression, apoptosis or cell differentiation, has led to a resurgence of interest in theoretical studies to establish the conditions under which bistability arises. Earlier theoretical studies identified two properties of signal transduction cascades as prerequisites for bistability: the existence of positive feedback loops and the cascade's intrinsic ultrasensitivity, which establishes a threshold for the activation of the feedback loop [12]. Here we analytically demonstrate that a double modification of a protein can generate bistability *per se* and we derive the necessary kinetic conditions to ensure that bistable behavior will be generated. Thus, analytic expressions for the bifurcation point as a function of the catalytic constants and Michaelis constants are given.

As a practical recipe and in summary, the presence of a double covalent modification enzyme cycle in a signal transduction network generates, *per se*, bistable behavior if the following prerequisites are satisfied: (a) one of the modifier enzymes catalyzes the two modification reactions or the two demodification reactions; (b) the ratio of the catalytic constants of the modification and demodification steps in the first modification cycle is less than this ratio in the second cycle; (c) the kinetics operate, at least in part, in the zero-order region. Thus, at least the enzyme that catalyzes the first step should be saturated by its substrate; for example, in step 1, e_1 should be saturated by α (Fig. 5D). This last condition is that which confers ultrasensitivity [4].

A double interconvertible cycle, which satisfies the three conditions described above, presents hysteresis. Therefore, the molar fraction variation of the three forms of the protein with respect to the change in the ratio of the modifier/demodifier enzymes ($T_{12} =$

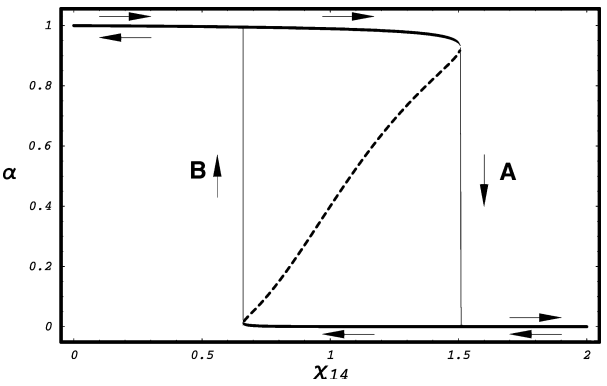

Fig. 9. Hysteresis behavior of the molar fraction α ($[W_\alpha]/W_T$) with respect to χ_{14} ($r_{14}e_{1T}/e_{2T}$) for a double modification/demodification interconvertible protein (Fig. 1). (A) Stable stationary state starting from $e_{T1} << e_{T2}$ ($\alpha = 1$). (B) Stable stationary state starting from $e_{T1} >> e_{T2}$ ($\alpha = 0$). The values of the parameters are $K_S = 0.01$ and $r_{31} = r_{24} = 2$. Note that the range of bistability behavior is (0.66, 1.51), whereas the range from the approximate expression given in Section 3.2, $[r_{24}(1 + K_S)/(\Theta(1 - 2K_S), r_{24}(1 - 2K_S)/(1 + K_S)]$, is (0.52, 1.94).

$e_{T1}/e_{T2} = \chi_{14}/r_{14}$) varies depending on the initial value of the enzyme ratio. For example, Fig. 9 shows the variation of the molar fraction α for two initial conditions, $e_{T1} << e_{T2}$, i.e. $\alpha = 1$ (curve A) and $e_{T1} >> e_{T2}$, i.e. $\alpha = 0$ (curve B). Starting at $e_{T1} << e_{T2}$ ($\alpha = 1$), the major flux is carried out by cycle 1 until the maximum value of e_{T1}/e_{T2} is achieved, before the flux passes to cycle 2. Conversely, if we start from $e_{T1} >> e_{T2}$ ($\alpha = 0$) the major flux is in cycle 2 until the minimum value of e_{T1}/e_{T2} is achieved (see Fig. 6A,D), before the flux passes to cycle 1. In these two cases, the control of the flux passes roughly from one cycle to the other when a critical value of χ_{14} is achieved.

The identification given in this article of the kinetic requirements necessary for a double modification enzyme to generate bistability *per se* offers a valuable tool to systematically analyze signal transduction networks and identify the modules that might generate bistability. Thus, the results reported here confirm that bistable system behavior can arise from the kinetics of double covalent modification of protein systems such as MAPK cascades, without the need to invoke the presence of any positive or negative feedback loops. Interestingly, kinetic data reported in the literature for the MAPK cascade show that some of its individual signaling elements could satisfy these requirements. In particular, for the double phosphorylation of MAPKK1 by p74raf-1, it has been reported by Alessi *et al.* [17] that the phosphorylation of the first site is the rate-limiting step and the phosphorylation of the second site then occurs extremely rapidly (i.e. $r_{31} >> 1$), so ensuring that the asymmetric factor ($\Theta = r_{31}r_{24}$) will be higher than 1 even if the two dephosphorylation steps occur at similar rates ($r_{24} \approx 1$). Thus, this experimental evidence suggests that the MAPKK1 modification cycle could behave as a bistable switch.

In Section 4 we also explored whether the presence of proteins that can be modified at more than two sites leads to the possibility of more complex behavior than bistability arising. We showed that multiple modification of a protein, even that catalyzed by the same enzyme, usually results in bistable behavior and not in multistability. However, we showed that the advantage of proteins with more than two modification sites is that the kinetic requirements to obtain bistability are less restrictive. Finally, we showed that the hierarchical organization of two double modification cycles can generate multistability *per se* without the existence of feedback or feedforward loops. As this hierarchical organization is ubiquitous in MAPK and other signal transduction pathways, this article also reports a new putative mechanism that *per se* explains multistability in signal transduction networks in which feedback or feedforward loops were not found experimentally. Multistability is linked to multifunction and crosstalk between signal transduction networks, which explains how the same signal transduction pathway can be responsible for the transduction of signals resulting in several different biological processes (e.g. apoptosis, cell growth and differentiation).

In conclusion, bistability and multistability can arise without the existence of feedback or feedforward loops, provided that some individual signaling elements are doubly modified proteins and the enzymes catalyzing these modifications follow a particular set of kinetic requirements. Therefore, the kinetic properties of two-step modification cycles, which are ubiquitous in signaling networks, could have evolved to support bistability and multistability, providing flexibility in the interchange between multistable and monostable modes. This analysis permits an explanation of multistability in systems in which feedback or feedforward loops were not found experimentally.

Acknowledgements

This study was supported by the Ministerio de Ciencia y Tecnología of the Spanish Government: SAF2005-9698 to MC and BQU2003-9698 to JLG and FM. The authors also acknowledge the support of the Bioinformatic grant program of the Foundation BBVA and the Comissionat d'Universitats i Recerca de la Generalitat de Catalunya. BNK acknowledges support from the National Institute of Health, Grant GM59570.

References

1 Ferrell JE Jr & Xiong W (2001) Bistability in cell signaling: How to make continuous processes discontinuous, and reversible processes irreversible. *Chaos* **11**, 227–236.
2 Bhalla US, Ram PT & Iyengar R (2002) MAP kinase phosphatase as a locus of flexibility in a mitogen activated protein kinase signalling network. *Science* **297**, 1018–1023.
3 Bhalla US & Iyengar R (1999) Emergent properties of networks of biological signalling pathways. *Science* **283**, 381–386.
4 Goldbeter A & Koshland DE Jr (1981) An amplified sensitivity arising from covalent modification in biological system. *Proc Natl Acad Sci USA* **78**, 6840–6844.
5 Koshland DE Jr, Goldbeter A & Stock JB (1982) Amplification and adaptation in regulatory and sensory systems. *Science* **217**, 220–225.
6 Huang CY & Ferrell JE Jr (1996) Ultrasensitivity in the mitogen-activated protein kinase cascade. *Proc Natl Acad Sci USA* **93**, 10078–10083.

7 Ferrell JE Jr (1996) Tripping the switch fantastic: how a protein kinase cascade can convert graded inputs into switch-like outputs. *Trends Biochem Sci* **21**, 460–466.
8 Ortega F, Acerenza L, Westerhoff HV, Mas F & Cascante M (2002) Product dependence and bifunctionality compromise the ultrasensitivity of signal transduction cascades. *Proc Natl Acad Sci USA* **99**, 1170–1175.
9 Laurent M & Kellershohn N (1999) Multistability: a major means of differentiation and evolution in biological systems. *Trends Biochem Sci* **24**, 418–422.
10 Sha W, Moore M, Chen K, Lassaletta AD, Yi C-S, Tyson JJ & Sible JC (2003) Hysteresis drives cell-cycle transitions in Xenopus laevis egg extracts. *Proc Natl Acad Sci USA* **100**, 975–983.
11 Tyson JJ, Chen CK & Novák B (2003) Sniffers, buzzers, toggles and blinkers: dynamics of regulatory and signaling pathways in the cell. *Curr Opin Cell Biol* **15**, 221–231.
12 Ferrell JE Jr (2002) Self-perpetuating states in signal transduction: positive feedback, double negative feedback and bistability. *Curr Opin Chem Biol* **6**, 140–148.
13 Thron CD (1997) Bistable biochemical switching and the control of the events of the cell cycle. *Oncogene* **15**, 317–325.
14 Lisman JE (1985) A mechanism for memory storage insensitive to molecular turnover: a bistable autophosphorylating kinase. *Proc Natl Acad Sci USA* **82**, 3055–3057.
15 Thomas R, Gathoye AM & Lambert L (1976) A complex control circuit. Regulation of immunity in temperature bacteriophages. *Eur J Biochem* **71**, 211–227.
16 Markevich NI, Hoek JB & Kholodenko BN (2004) Signaling switches and bistability arising from multisite phosphorylation in protein kinase cascades. *J Cell Biol* **164**, 353–359.
17 Alessi DR, Saito Y, Campbell DG, Cohen P, Sithanandam G, Rapp U, Ashworth A, Marshall CJ & Cowley S (1994) Identification of the sites in MAP kinase kinase-1 phosphorylated by p74raf-1. *EMBO J* **13**, 1610–1619.
18 Ferrell JE Jr & Bhatt RR (1997) Mechanistic studies of the dual phosphorylation of mitogen-activated protein kinase. *J Biol Chem* **272**, 19008–19016.

Appendix A: Kinetic derivation

In line with the terms used in the main text, the concentration–conservation relationships for the interconversion, shown in Fig. 1, are as follows:

$$\begin{aligned} W_T &= [W_\alpha] + [W_\beta] + [W_\gamma] + [e_1W_\alpha] + [e_1W_\beta] \\ &\quad + [e_2W_\gamma] + [e_2W_\beta], \\ e_{1T} &= [e_1] + [e_1W_\alpha] + [e_1W_\beta], \\ e_{2T} &= [e_2] + [e_2W_\gamma] + [e_2W_\beta]. \end{aligned} \tag{A1}$$

where e_1W_α, e_1W_β, e_2W_β and e_2W_γ are the M-M complexes. W_T and e_{iT} are the total concentration of the interconvertible protein and the total concentration of the catalyst, respectively. Note that only the formation of substrate–enzyme complexes, and not product–enzyme complexes, was considered.

Under the steady-state assumption, the rate equations (v_i) have the following form for the four steps:

$$\begin{aligned} v_1 &= \frac{V_{m1}\frac{[W_\alpha]}{K_{m1}}}{1+\frac{[W_\alpha]}{K_{m1}}+\frac{[W_\beta]}{K_{m3}}}, \quad v_3 = \frac{V_{m3}\frac{[W_\beta]}{K_{m3}}}{1+\frac{[W_\alpha]}{K_{m1}}+\frac{[W_\beta]}{K_{m3}}} \\ v_2 &= \frac{V_{m2}\frac{[W_\beta]}{K_{m2}}}{1+\frac{[W_\gamma]}{K_{m4}}+\frac{[W_\beta]}{K_{m2}}}, \quad v_4 = \frac{V_{m4}\frac{[W_\gamma]}{K_{m4}}}{1+\frac{[W_\gamma]}{K_{m4}}+\frac{[W_\beta]}{K_{m2}}} \end{aligned} \tag{A2}$$

K_{mi} $[(k_{di} + k_i)/k_{ai}]$ is the Michaelis constant and V_{mi} $(k_i e_{jT}, i = 1, 4)$ is the maximal rate of each of the four steps, where $j = 1$ for $i = 1, 3$ and $j = 2$ for $i = 2, 4$.

To simplify the mathematical manipulation, we make the concentration of the variables W_α, W_β and W_γ dimensionless. The dimensionless concentrations of the variables are $\alpha = [W_\alpha]/W_T$, $\beta = [W_\beta]/W_T$ and $\gamma = [W_\gamma]/W_T$. Thus, α, β and γ belong to the range 0, 1. Additionally, we normalize the Michaelis constants in such a way that $K_{S1} = K_{m1}/W_T$, $K_{S2} = K_{m2}/W_T$, $K_{S3} = K_{m3}/W_T$ and $K_{S4} = K_{m4}/W_T$. On introducing these new dimensionless variables into the previous rate equations we obtain:

$$\begin{aligned} v_1 &= \frac{V_{m1}\frac{\alpha}{K_{S1}}}{1+\frac{\alpha}{K_{S1}}+\frac{\beta}{K_{S3}}} \quad v_3 = \frac{V_{m3}\frac{\beta}{K_{S3}}}{1+\frac{\alpha}{K_{S1}}+\frac{\beta}{K_{S3}}} \\ v_2 &= \frac{V_{m2}\frac{\beta}{K_{S2}}}{1+\frac{\gamma}{K_{S4}}+\frac{\beta}{K_{S2}}} \quad v_4 = \frac{V_{m4}\frac{\gamma}{K_{S4}}}{1+\frac{\gamma}{K_{S4}}+\frac{\beta}{K_{S2}}} \end{aligned} \tag{A3}$$

Appendix B: Visualization of the bifurcation point

In Section 2, we have shown that the system represented by Fig. 1 can display bistable behavior. Here, we describe in detail the procedure for deducing the conditions at which the system changes qualitatively its behavior from one to two stable steady-states, i.e. the bifurcation point.

For the sake of simplicity, we assume that the Michelis constants of both enzymes are equal ($K_{S1} = K_{S2} = K_S$). For this case, Eqn (4) is:

$$\chi_{14} = \frac{\beta\gamma + \beta^2\Theta + \gamma K_S}{\beta r_{31}(\beta + \gamma + K_S)} \tag{A4}$$

This equation explicitly indicates the relationship between the fraction χ_{14} and the normalized concentration form γ. Using this equation, the variation of χ_{14}

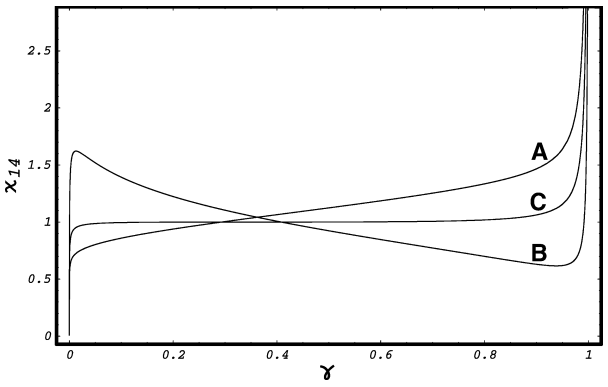

Fig. B1. Variation of χ_{14} with respect to γ for three different values of the parameters. (A) $\Theta = 1/2$ and $r_{31} = 1\sqrt{2}$. (B) $\Theta = 4$ and $r_{31} = 2$. (C) $\Theta = 1.062$ and $r_{31} = 1.031$.

with γ for different values of the asymmetric factor ($\Theta = r_{31}\, r_{24}$) and $K_S = 10^{-2}$ is shown in Fig. B1. Thus, for Θ equal to 0.5, this curve increases monotonically with γ, i.e. $\delta\gamma/\delta\chi_{14} > 0$ (curve A). However, for a higher value of the asymmetric factor, e.g. $\Theta = 4$, the sign of the slope depends on the γ value, and the curve displays two extrema points, and then the sign of the slope curve changes with the γ value (curve B). Between these two types of behavior, there should be one intermediate condition for a Θ value in which the two extremes and the inflection point coincide, i.e. $\left(\frac{\partial\chi_{14}}{\partial\gamma}\right) = 0$ and $\left(\frac{\partial^2\chi_{14}}{\partial\gamma^2}\right) = 0$ for a given γ value (curve C). Calculating the first derivative we obtain:

$$\left(\frac{\partial\,\chi_{14}}{\partial\gamma}\right) = 2\,\mathrm{K_s}(1+\mathrm{K_s})\Theta^2 + (\Theta - 1 + \mathrm{K_s}(4\Theta - 1) \times \gamma((2\Theta - 1)\,\gamma - 2\Theta) + \sqrt{\gamma(4\Theta + \gamma - 4\Theta\,\gamma)} \times (\Theta - 1 + \mathrm{K_s}(4\Theta - 1))\gamma$$

Equating this expression to zero, four values of γ are obtained:

$$\gamma_{1,2} = \frac{1}{2}\left(1 - \frac{\sqrt{\mathrm{K_s}}\sqrt{1+\mathrm{K_s}}}{\sqrt{\Theta - 1 + \mathrm{K_s}(4\Theta - 1)}} \pm \sqrt{\mathrm{A}}\right)$$

and

$$\gamma_{3,4} = \frac{1}{2}\left(1 + \frac{\sqrt{\mathrm{K_s}}\sqrt{1+\mathrm{K_s}}}{\sqrt{\Theta - 1 + \mathrm{K_s}(4\Theta - 1)}} \pm \sqrt{\mathrm{A}}\right)$$

where

$$\mathrm{A} = \frac{\Theta - 1 + \mathrm{K_s^2}(-4\Theta + 1) - 2\sqrt{\mathrm{K_s}}\sqrt{1+\mathrm{K_s}}\sqrt{\Theta - 1 + \mathrm{K_s}(4\Theta - 1)}}{\Theta - 1 + \mathrm{K_s}(4\Theta - 1)}$$

For example, since curve (A) (Fig. B1) is monotonous, these four roots take imaginary values, i.e. $A < 0$. On the contrary, curve (B) presents two turning points; A should then be greater than 0 and the system presents two different root values in the range [0, 1], i.e. $0 < \gamma_1 < 1$ and $0 < \gamma_2 < 1$; meanwhile, the $\gamma_{3,4}$-values have no physical meaning. Curve (C) (Fig. B1) has one double root ($\gamma_1 = \gamma_2$) and then $A = 0$; the values of the other roots $\gamma_3 = \gamma_4$ acquire a nonsignificant physical meaning. The parameter value that fulfils the condition $A = 0$ is as follows: $\Theta = (1 + K_S)^2/(1 - 2K_S)^2$. This Θ value occurs at the bifurcation point. At this point, the solutions with physical meaning for γ only are $\gamma_{1,2} = \frac{1+\mathrm{K_s}}{3}$ It can be easily shown that this condition makes the second derivative $\left(\frac{\partial^2\chi_{14}}{\partial\gamma^2}\right) = 0$. In addition, substituting the expressions in the equations described above gives $\alpha = \gamma = \frac{1+\mathrm{K_s}}{3}$ and $\beta = \frac{1-2\mathrm{K_s}}{3}$.

Supplementary material

The following supplementary material is available online:

Doc. S1. (A) Bifurcation point derivation for different Michaelis constants. (B) Maximum values of some variables assuming equal Michaelis constants. (C) Multistable behaviour in a cascade of two modifier cycles.

Fig. S1. Variation of the steady-state molar fraction of the interconvertible protein Z, in the form $Z\gamma$, in terms of χ_{18} for the model described in Fig. 8b. The parameters are Θ_W ($r_{31}r_{24}$) = 30 and Θ_Z ($r_{75}r_{68}$) = 50 for the first and second double modification cycles, respectively and $K_S = 10^{-2}$.

This material is available as part of the online article from http://www.blackwell-synergy.com